LIMITATIONS IN APPLICATION OF FINITE ELEMENT METHOD IN ACOUSTIC NUMERICAL SIMULATION

Tomasz Łodygowski
Wojciech Sumelka

Faculty of Civil and Environmental Engineering, Poznan University of Technology
e-mail: Tomasz.Lodygowski@put.poznan.pl; Wojciech.Sumelka@ikb.poznan.pl

In the paper, we introduce information on limitations of the Finite Element Method in acoustic analysis. Difficulties that appear in acoustic analysis are mainly caused by the form of shape functions and sensitivities to boundaries, so we start with a short description of mathematical background. The propositions how to overcome and simplify those disadvantages are summarized and illustrated with a real application.

Key words: applied acoustics, finite element method

1. Introduction

Although the fundamental part of the mathematical description of the acoustic wave was created more than one hundred years ago (Strutt, 1945), the problem of the effective solution to the wave equation in connection with arbitrary domains, boundary conditions and initial conditions is still vivid.

In general, the partial differential wave equation can be solved only with using numerical methods. There are several possibilities, and the decision on which type of a numerical tool should be used is strictly determined by the frequency of the acoustic wave.

Acoustic problems can be divided into three main groups according to the wave frequency order (Rabbiolo *et al.*, 2004):

Low frequency problems: the response exhibits strong modal behavior,

Medium frequency problems: the response spectra exhibit high irregularities, indicating irregular modal density. Boundary conditions, geometry and materials play the fundamental role.

High frequency problems: the response spectra are "smooth", indicating high modal "density". Boundary conditions, geometry and materials are not important.

The first and the second type of analysis can be efficiently solved using Boundary Element Method (BEM), and especially Finite Element Method (FEM). The third one, i.e. high frequency problems can be solved on the basis of Statistical Energy Analysis (SEA).

2. Mathematical formulation

2.1. General formulation

The FEM equations are obtained from the equilibrium equation for small motions of a compressible adiabatic fluid with velocity-dependent momentum losses in the form [1]

$$\frac{\partial p}{\partial \boldsymbol{x}} + \gamma(\boldsymbol{x}, \theta_i)\dot{\boldsymbol{u}}^f + \rho_f(\boldsymbol{x}, \theta_i)\ddot{\boldsymbol{u}}^f = 0 \qquad (2.1)$$

where p is the excess pressure in the fluid (the pressure in excess of any static pressure), $\boldsymbol{x}$ is the spatial position of the fluid particle, $\dot{\boldsymbol{u}}^f$ is the fluid particle velocity, $\ddot{\boldsymbol{u}}^f$ is the fluid particle acceleration, ρ_f is the density of the fluid, γ is the "volumetric drag" (force per unit volume per velocity), and θ_i are i independent field variables such as temperature, humidity of air, or salinity of water on which ρ_f and γ may depend.

The constitutive behavior of the fluid is assumed to be inviscid, linear and compressible, so

$$p = -K_f(\boldsymbol{x}, \theta_i)\frac{\partial}{\partial \boldsymbol{x}} \cdot \boldsymbol{u}^f \qquad (2.2)$$

where K_f is the bulk modulus of the fluid.

The weak form of Eq. (2.1) (the integral one for an arbitrary variational field δp) after using Green's theorem and substituting the constitutive law, has the final shape for a continuous domain

$$\int\limits_{V_f} \left[\delta p\Big(\frac{1}{K_f}\ddot{p} + \frac{\gamma}{\rho_f K_f}\dot{p}\Big) + \frac{1}{\rho_f}\frac{\partial}{\partial \boldsymbol{x}}\delta p \cdot \frac{\partial}{\partial \boldsymbol{x}}p\right] dV - \int\limits_{S} \delta p(T(\boldsymbol{x}))\, dS = 0 \qquad (2.3)$$

where

$$T(\boldsymbol{x}) = -\boldsymbol{n} \cdot \Big(\frac{1}{\rho_f}\frac{\partial}{\partial \boldsymbol{x}}p\Big)$$

and the vector $\boldsymbol{n}$ represents the *inward* normal to the acoustic medium at the boundary.

2.2. Boundary conditions

The last term in Eq. (2.3) introduces the boundary condition statement for acoustic problems. All of boundary conditions described below can be formulated in terms of $T(\boldsymbol{x})$ – this term has dimensions of acceleration. Dividing the boundary into subregions S, the following conditions can be imposed [1]:

— S_{fp}: where the value of acoustic pressure p is prescribed ($\delta p = 0$)

$$T(\boldsymbol{x}) = \boldsymbol{n} \cdot \left(\ddot{\boldsymbol{u}}^f + \frac{\gamma}{\rho_f} \dot{\boldsymbol{u}}^f \right) \tag{2.4}$$

— S_{ft}: where the inward acceleration of the acoustic medium is prescribed ($\gamma = 0$)

$$T(\boldsymbol{x}) = \boldsymbol{n} \cdot \ddot{\boldsymbol{u}}^f \tag{2.5}$$

— S_{fs}: the acoustic-structural boundary, where the acoustic and structural media have the same displacement normal to the boundary

$$T(\boldsymbol{x}) = \boldsymbol{n} \cdot \left(\ddot{\boldsymbol{u}}^m + \frac{\gamma}{\rho_f} \dot{\boldsymbol{u}}^m \right) \tag{2.6}$$

$\boldsymbol{u}^m$ denotes the displacement of the structure,

— S_{fr}: the reactive acoustic boundary – admittance conditions are applied

$$T(\boldsymbol{x}) = -\left[\frac{\gamma}{\rho_f} \frac{1}{c_1} p + \left(\frac{\gamma}{\rho_f} \frac{1}{k_1} + \frac{1}{c_1} \right) \dot{p} + \frac{1}{k_1} \ddot{p} \right) \tag{2.7}$$

where the inverse of $1/k_1$ and $1/c_1$ are the spring and dashpot parameters, respectively,

— S_{frs}: the mixed impedance boundary and acoustic-structural boundary

$$T(\boldsymbol{x}) = -\left[\frac{\gamma}{\rho_f} \frac{1}{c_1} p + \left(\frac{\gamma}{\rho_f} \frac{1}{k_1} + \frac{1}{c_1} \right) \dot{p} + \frac{1}{k_1} \ddot{p} \right] + \boldsymbol{n} \cdot \left(\ddot{\boldsymbol{u}}^m + \frac{\gamma}{\rho_f} \dot{\boldsymbol{u}}^m \right) \tag{2.8}$$

— S_{fi}: the "infinite" boundary conditions, obtained from using infinite elements or from a proper choice of impedance coefficients. For the second proposal, it can be written

$$T(\boldsymbol{x}) = -\left(\frac{1}{c_1} \dot{p} + \frac{1}{a_1} p \right) \tag{2.9}$$

— S_{ff}: the boundary between acoustic fluids of possibly different material properties.

2.3. Formulation for transient response

Using Eqs. (2.4)-(2.9) in Eq. (2.3), the final variational statement for the acoustic medium is obtained in the following form

$$
\int_{V_f} \left[\delta p \Big(\frac{1}{K_f} \ddot{p} + \frac{\gamma}{\rho_f K_f} \dot{p} \Big) + \frac{1}{\rho_f} \frac{\partial}{\partial \boldsymbol{x}} \delta p \cdot \frac{\partial}{\partial \boldsymbol{x}} p \right] dV +
$$

$$
+ \int_{S_{fr}} \delta p \left[\frac{\gamma}{\rho_f} \frac{1}{c_1} p + \Big(\frac{\gamma}{\rho_f} \frac{1}{k_1} + \frac{1}{c_1} \Big) \dot{p} + \frac{1}{k_1} \ddot{p} \right] dS +
$$

$$
+ \int_{S_{fi}} \delta p \Big(\frac{1}{c_1} \dot{p} + \frac{1}{a_1} p \Big) dS - \int_{S_{fs}} \delta p (\boldsymbol{n} \cdot \ddot{\boldsymbol{u}}^m) \, dS + \tag{2.10}
$$

$$
+ \int_{S_{frs}} \delta p \left[\frac{\gamma}{\rho_f} \frac{1}{c_1} p + \Big(\frac{\gamma}{\rho_f} \frac{1}{k_1} + \frac{1}{c_1} \Big) \dot{p} + \frac{1}{k_1} \ddot{p} \right] dS +
$$

$$
- \int_{S_{frs}} \delta p (\boldsymbol{n} \cdot \ddot{\boldsymbol{u}}^m) \, dS - \int_{S_{ft}} \delta p (\boldsymbol{n} \cdot \ddot{\boldsymbol{u}}^f) \, dS = 0
$$

For the acoustic-structural coupling, assuming that the structural behavior is defined by the virtual work in the form

$$
\int_V \delta \boldsymbol{\varepsilon} : \boldsymbol{\sigma} \, dV + \int_V \alpha_c \rho \delta \boldsymbol{u}^m \cdot \dot{\boldsymbol{u}}^m \, dV + \int_V \rho \delta \boldsymbol{u}^m \cdot \ddot{\boldsymbol{u}}^m \, dV +
$$

$$
\tag{2.11}
$$

$$
- \int_{S_t} \delta \boldsymbol{u}^m \cdot \boldsymbol{t} \, dS + \int_{S_{fs}} p \delta \boldsymbol{u}^m \cdot \boldsymbol{n} \, dS = 0
$$

where σ is the stress at a point in the structure, p is the pressure acting on the fluid-structural interface, $\boldsymbol{n}$ is the outward normal to the structure, ρ is the density of the material, $\boldsymbol{t}$ is the surface traction and $\delta \varepsilon$ and $\delta \boldsymbol{u}^m$ are strain variation and variational displacement field, respectively. The final FEM equation (after linearization) in a matrix notation is

$$
- \delta \widehat{p}^P \{ (M_f^{PQ} + M_{fr}^{PQ}) \ddot{p}^Q + (C_f^{PQ} + C_{fr}^{PQ}) \dot{p}^Q +
$$

$$
+ (K_f^{PQ} + K_{fr}^{PQ} + K_{fi}^{PQ}) p^Q - S_{fs}^{PM} \ddot{u}^M - P_f^P \} + \tag{2.12}
$$

$$
+ \delta u^N \{ I^N + M^{NM} \ddot{u}^M + C_{(m)}^{NM} \dot{u}^M + (S_{fs}^{QN})^\top p^Q - P^N \} = 0
$$

where $\delta p^P = d^2 (\delta \widehat{p}^P)/dt^2$.

In Eg. (2.12), a semidiscrete approximation is assumed and the pressure and displacement fields are interpolated as follows

$$
p = H^P p^P \qquad \boldsymbol{u}^m = N^N u^N \tag{2.13}
$$

where $p = 1, 2, \ldots$ up to the number of pressure nodes and $N = 1, 2, \ldots$ up to the number of displacement degrees of freedom (for detailed information see Sumelka, 2004).

2.4. Formulation for steady-state response

For steady-state analysis, we assume that all degrees of freedom and loads vary harmonically at the angular frequency Ω, so in general for an arbitrary variable field we can write

$$f = \widetilde{f} \exp \mathrm{i}\Omega t \qquad (2.14)$$

where $\widetilde{f}$ denotes a constant complex amplitude.

By analogy to Eq. (2.3) and using the basic assumption (Eq. (2.14)) we obtain

$$-\int_{V_f} \delta p \frac{\Omega^2}{K_f} \widetilde{p}\, dV + \int_{V_f} \frac{1}{\widetilde{\rho}} \frac{\partial}{\partial \boldsymbol{x}} \delta p \cdot \frac{\partial}{\partial \boldsymbol{x}} \widetilde{p}\, dV - \int_S \delta p \widetilde{T}(\boldsymbol{x})\, dS = 0 \qquad (2.15)$$

where

$$\widetilde{T}(\boldsymbol{x}) = -\frac{1}{\widetilde{\rho}} \frac{\partial}{\partial \boldsymbol{x}} \widetilde{p} \cdot \boldsymbol{n}$$

and

$$\widetilde{\rho} \equiv \rho_f + \frac{\gamma}{\mathrm{i}\Omega}$$

is the complex density.

After applying an analogous form of boundary conditions as for the transient one, the final variational statement for steady-state analysis becomes

$$\int_{V_f} \left[-\Omega^2 \delta p \Big(\frac{1}{K_f} \widetilde{p} \Big) + \frac{1}{\widetilde{\rho}} \frac{\partial}{\partial \boldsymbol{x}} \delta p \cdot \frac{\partial}{\partial \boldsymbol{x}} \widetilde{p} \right] dV + \int_{S_{ft}} \Omega^2 \delta p \boldsymbol{n} \cdot \widetilde{\boldsymbol{u}}^f\, dS +$$

$$+ \int_{S_{fr} \cup S_{fi}} \delta p \Big(\frac{\mathrm{i}\Omega}{c_1} - \frac{\Omega^2}{k_1} \Big) \widetilde{p}\, dS + \int_{S_{frs}} \delta p \Big(\frac{\mathrm{i}\Omega}{c_1} \widetilde{p} - \frac{\Omega^2}{k_1} \widetilde{p} + \Omega^2 \boldsymbol{n} \cdot \widetilde{\boldsymbol{u}}^m \Big)\, dS + (2.16)$$

$$+ \int_{S_{fs}} \Omega^2 \delta p \boldsymbol{n} \cdot \widetilde{\boldsymbol{u}}^m\, dS = 0$$

The final FEM equation for steady-state problems, as for the transient one, for acoustic-structural coupling we introduce by comparison to Eq. (2.15) and Eq. (2.11) in the form

$$-\delta \widehat{p}^P \{ [-\Omega^2 (M_f^{PQ} + M_{fr}^{PQ}) + \mathrm{i}\Omega (C_f^{PQ} + C_{fr}^{PQ}) + K_f^{PQ}] \Delta \widetilde{p}^Q + \Omega^2 S_{fs}^{PM} \Delta \widetilde{u}^M +$$

$$-\Delta \widetilde{P}_f^P \} + \delta u^N \{ [-\Omega^2 M^{NM} + \mathrm{i}\Omega (C_{(m)}^{NM} + C_{(k)}^{NM}) + K^{MN}] \Delta \widetilde{u}^M + \qquad (2.17)$$

$$+ (S_{fs}^{QN})^\top \Delta \widetilde{p}^Q - \Delta \widetilde{P}^N \} = 0$$

where

$$\delta\widetilde{p}^P = -\Omega^{-2}\delta p^P$$

$$\Delta\widetilde{p}^Q = [\Re(\widetilde{p}^Q) + i\Im(\widetilde{p}^Q)]\exp(i\Omega t)$$

$$\Delta\widetilde{u}^M = [\Re(\widetilde{u}^M) + i\Im(\widetilde{u}^M)]\exp(i\Omega t)$$

$$\Delta\widetilde{P}^N = [\Re(\widetilde{P}^N) + i\Im(\widetilde{P}^N)]\exp(i\Omega t)$$

$$\Delta\widetilde{P}_f^P = [\Re(\widetilde{P}_f^P) + i\Im(\widetilde{P}_f^P)]\exp(i\Omega t)$$

The terms $\Re(\widetilde{p}^Q)$, $\Re(\widetilde{u}^M)$, $\Im(\widetilde{p}^Q)$ and $\Im(\widetilde{u}^M)$ are the real and imaginary parts of the amplitudes of the response; $\Re(\widetilde{P}^N)$ and $\Im(\widetilde{P}^N)$ are the real and imaginary parts of the amplitude of the force applied to the structure; $\Re(\widetilde{P}_f^P)$ and $\Im(\widetilde{P}_f^P)$ are the real and imaginary parts of the amplitude of the acoustic traction applied to the fluid (see also Sumelka, 2004).

3. Limitations in using FEM

3.1. Choosing proper element size

The crucial point in the present most popular finite element applications is that the shape functions are linear or quadratic. Such an approximation, sufficient in most engineering applications, in acoustic analysis, where the frequency of excitations change from several to over a dozen thousand hertzs, determines the delimitation of applicability of the above mentioned method.

There is a strong relationship between the wave frequency and finite element size. The approximation for the pressure field, imposed in Eq. $(2.13)_1$, introduces linear or quadratic shape functions H. To obtain acceptable results, the following requirements must be fulfilled [1]. For the first order elements (linear shape functions), the element dimensions have to be chosen such that the biggest one is at least six times smaller than the acoustic wavelength. For the second order elements, this requirement is twice smaller.

To understand how fast such requirements can cause that hardware possibilities are exceeded, let us introduce a simple example. Let imagine a typical room of dimensions $2.5 \times 2.5 \times 3.0$ m. Assuming that computations have to cover the frequency range from 100 Hz to 10 kHz with the using first order elements used, the total number of finite elements needed in analysis is as follows. For room temperature, in the case when frequency of excitation reaches 100 Hz the biggest element dimension should not exceed 0.57 m, so ~ 100 elements need to be used. But for frequency 10 kHz, the maximal element dimension is 0.57 mm, and the total number of finite elements reaches ~ 100 m.

The problem of proper dimensions of the dements is even more complicated if there is a possibility of wave reflection or interference of waves in the model. In such situations, we cannot predict *a priori* the frequency of the resultant wave, so the solution can be obtained in an iterative process only.

3.2. Defining absorptive boundary conditions

Results of numerical analysis of wave propagation phenomena are very sensitive to boundary conditions. Appropriate conditions have to ensure that all physical phenomena connected with waves like reflection, absorption or transmission are correctly defined.

Eq. (2.7) introduces one of the most important boundary terms. The "absorption" coefficients (k_1 and c_1) enable one to obtain demanded reflection conditions from total absorption to total reflection. Unfortunately, those coefficients are not given by supplier of the acoustic material. What is more, the "absorption" at the boundary is nonlinearly dependent on wave frequency. The factors k_1 and c_1 should be then functions of frequency, which, in general, is not implemented in popular finite element systems. The proposition how to manage with the first of the above mentioned disadvantage is shown in Sumelka (2004).

Another serious limitation is that the absorptive properties of materials are not only caused by physical properties themselves. The shape of boundaries plays crucial role in the process of acoustic wave energy dissipation, Fig. 1. The exact mapping of such complicated boundaries would result in a large number of additional variables, so the process of boundary homogenization is needed (for detailed discussion see Sumelka ans Łodygowski (2004)).
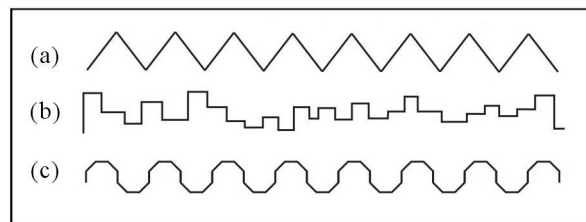

Fig. 1. A cross section through a typical acoustic material: (a) pyramid, (b) rectangular prism, (c) other

4.   Example

4.1.   Assembly hall "MAGNA"

Assembly hall "MAGNA" is the central point of the Educational Center (see Fig. 2) at Poznan University of Technology (PUT).
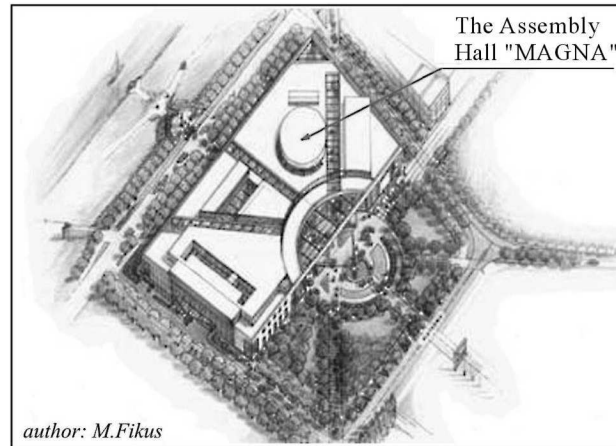

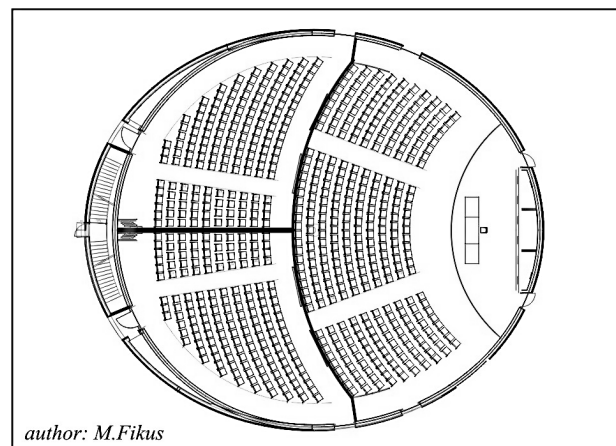Fig. 2. A general view of PUT Educational Center

Fig. 3. A horizontal cross section of hall "MAGNA"

The main task of "MAGNA" hall is to create representative place for PUT ceremonies, international symposia and conferences, concertos and even movie shows. During an academic year, the assembly hall is an auditorium for students. The most interesting thing is that the whole area of "MAGNA" hall can be divided into three separate areas by using special "moving" walls,

so three independent audiences can be obtained, Fig. 3 (thick line indicates borderline).

In a horizontal cross section "MAGNA" hall is an ellipse (see Fig. 3), whose major axis is 33.85 m and the minor axis is 29.53 m with total area 691 m^2. In the top-most point there is nearly 10 m (see Fig. 4). The total volume of the assembly hall is about 6750 m^3.
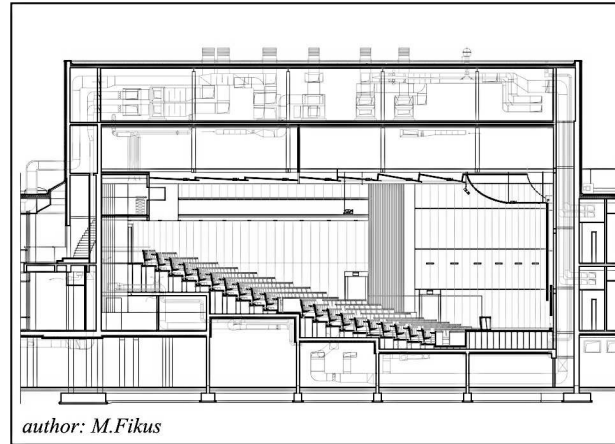

author: M.Fikus

Fig. 4. A vertical cross section through the major axis

The elliptic shape of the assembly hall is not optimal in the sense of acoustic properties because it is similar to a huge mirror which concentrates reflected waves at the center of "MAGNA". That is why all surfaces at the rear (the walls and a part of ceiling) have to assure absorptive conditions (absorption coefficient $\alpha \approx 0.8$)[1].

In the experimental tests and numerical analysis the possibility of division the area of "MAGNA" hall into three separated auditoria was omitted due to the fact that the structural integrity of the assembly hall has been a priority.

4.2. Numerical analysis

The 3D and 2D numerical models of assembly hall "MAGNA" are shown in Fig. 5 and Fig. 6, respectively. Because of the above mentioned great sensitivity to the boundary shape in acoustic analysis, all details in geometry such as complexity of ceiling, stairs, seats, stage, etc. were mapped with high precision.

Due to the strong relationship between the length of acoustic wave and element dimensions, precisely described in Section 3.1, the analysis of a three dimensional model was impossible.

---

[1]The complete information about the problems of the Architectural Acoustic can be found in Sadowski (1971, 1976), Sadowski and Wodziński (1959).
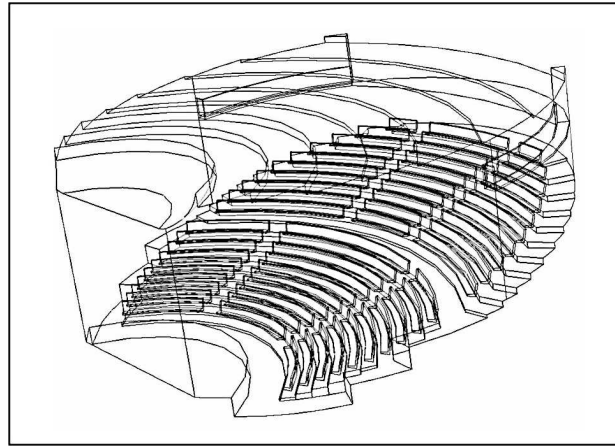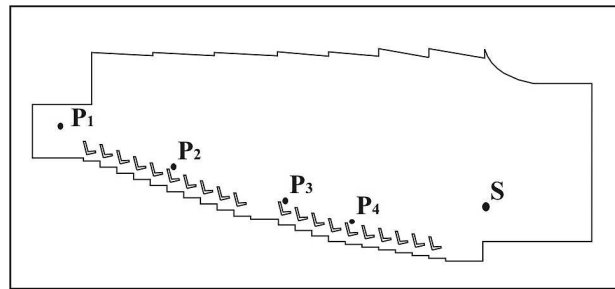
Fig. 5. A 3D model of assembly hall "MAGNA"

Fig. 6. A 2D model of assembly hall "MAGNA" – a cross section through the major axis

The total volume of the assembly hall is about $6750\,\mathrm{m}^3$, as mentioned. Considering the complexity of geometry of "MAGNA" hall, it can be easily shown that the minimal dimensions of the cubic finite element are about $0.2\,\mathrm{m}$, so the minimal number of finite elements required reaches $800k$. On the basis of Section 3.1, the above mentioned mesh density is suitable up to $\sim 500\,\mathrm{Hz}$ for elements with quadratic shape function, and up to $\sim 250\,\mathrm{Hz}$ for elements with linear shape function. The relation between frequency and required number of finite elements is inversely proportional to the cube of frequency in 3D acoustic simulations, so it can be easily computed that for analysis with the highest frequency acceptable by human sense of hearing, i.e. $20\mathrm{k}\,\mathrm{Hz}$, the total number of elements would be nearly $200\,\mathrm{G}$.

Such high computational requirements caused that a substitutive two-dimensional model of the assembly hall was prepared (Fig. 6). The 2D model was a cross section of the 3D model cut through the major axis with the total area of about $260\,\mathrm{m}^2$. The maximum number of required finite elements at the

whole range of frequency, i.e. from 16 Hz-20 kHz, was then 10 m (for second order elements).

Two-dimensional modeling of "MAGNA" hall has a lot of disadvantages which limit the applicability of such an approach. A three dimensional interpretation of the 2D model is an infinitely long "tube" (Fig. 7), so it was impossible to model the reflection from the left and right sides, and in consequence, computations of the steady state-response or self response were not feasible.
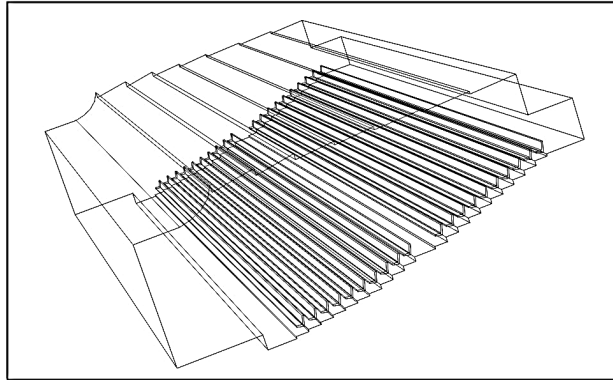

Fig. 7. A 2D model interpretation

The only way was to execute the numerical simulations as transient ones. The duration of the analysis step had to guarantee that the wave reflected from the left and right sides would not reach the analyzed cross section.

We decided to divide the analysis into two steps. In the first step, the time needed to travel a distance from the source to lateral walls and back to the major axis by an acoustic wave was investigated. In the second step (the principal), the essential computations were made during the time determined in the first step. In each analysis step we assumed that the room temperature is considered, so the following values describing the acoustic medium were established: the density of air $\rho_f = 1.20 \, \text{kg/m}^3$, and the bulk modulus $K_f = 141.8 \, \text{kN/m}^2$.

Computations were made using ABAQUS Explicit system (based on explicit integration method).

First step. An additional model was created. The model was a horizontal cross section of the assembly hall at the level of the center of spherical source (Fig. 8).

The results showed that the time needed to travel a distance from the source to lateral walls and back to the major axis by an acoustic wave reached

Fig. 8. Acoustic pressure [Pa] – the investigation of the second step time duration

~ 0.1 s. This time was recognized as a time in which the results obtained from the two-dimensional model (from second step) should have satisfied accuracy.

Second step. The scheme of the model with marked measure points P_i and source S is shown in Fig. 6. The length of the model (identical to the major axis) is 33.85 m, and in the top-most point the height is nearly 10.00 m.

The 2D model was meshed by four node linear elements (in ABAQUS notation AC2D4R) whose average dimensions were ~ 0.1 m. Such mesh density ($40k$ dof) enabled one to lead computations for frequencies up to 500 Hz.

It is important to notice that due to the fact that human sense of hearing accepts the sound pressure from $2 \cdot 10^{-5}$ Pa ($0dB$ – threshold of hearing) up to 20 Pa ($120dB$ – pain threshold), the local results has qualitative meaning in acoustic analysis. The contour maps of acoustic pressure distribution gives a general view of the solution obtained (Fig. 9).

Fig. 9. A contour map of acoustic pressure distribution [Pa] for 200 Hz

The detailed information about analysis is placed in following Section 4.4, where a comparison between the numerical simulations and experimental tests is presented.

4.3. Experiment tests

To validate the results obtained in computations of the mathematical model, experimental tests were carried out. A precise description of the experiment and test equipment is presented below. The acoustical experiment was prepared before the Educational Center was opened, on a holiday, so the results were free of incidental noise.

Measurement equipment. The wave source consisted of the following: wave generator "Metatronik" G430, frequency counter "ALFA Electonics" FC-1200, amplifier "Luxman Amplifier" LV102 and sphere loudspeaker. The acoustic signal was recorded by a microphone connected with oscilloscope "LeCroy" 9310M and handheld sound and vibration analyser "SVANTEK" SVAN 912AE. The signal was calibrated by sound level calibrator KA-10.

Measurement process. The experimental tests were executed in the following way. The stationary spherical source S was placed on the major axis, by analogy to numerical analysis. Measurement points P_i were situated on the level of a human head while seated (Fig. 6). A sinusoidal signal was generated at a range from $150\,\text{Hz}$ to $700\,\text{Hz}$ with the step $50\,\text{Hz}$, and the sound level run from $98dB$ to $107dB$ dependently on frequency.
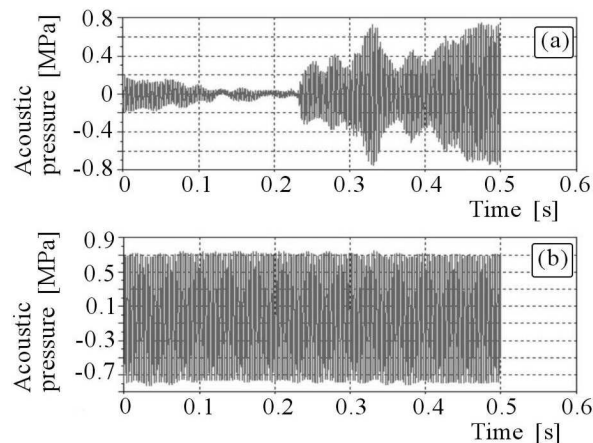

Fig. 10. Results at the point P_3 for frequency $300\,\text{Hz}$: (a) transient case,
(b) steady-state case

At each point and at each frequency of interest two kinds of readings were made. The first one enabled one to observe the moment in which the acoustic wave was reaching the measure point and the second one enabled observation

of the steady-state response (Fig. 10). The individual reading was 0.5 s long with the time sampling $1 \cdot 10^{-5}$ s.

A graphical representation of the output data was prepared in a free scientific software package for numerical computations *SciLab 3.0.*

4.4.   Comparison

The comparison between the numerical analysis and experimental tests is shown in Fig. 11 and Fig. 12. These figures indicate differences in the acoustic pressure [Pa] from 0 s to 0.1 s. The first appearance of the acoustic wave in the measurement points can be observed. A mathematical idealization of the results in the artificial zero pressure before the acoustic wave came in (black line).

The mesh density applied to the model should gave satisfactory results up to 500 Hz, as mentioned.
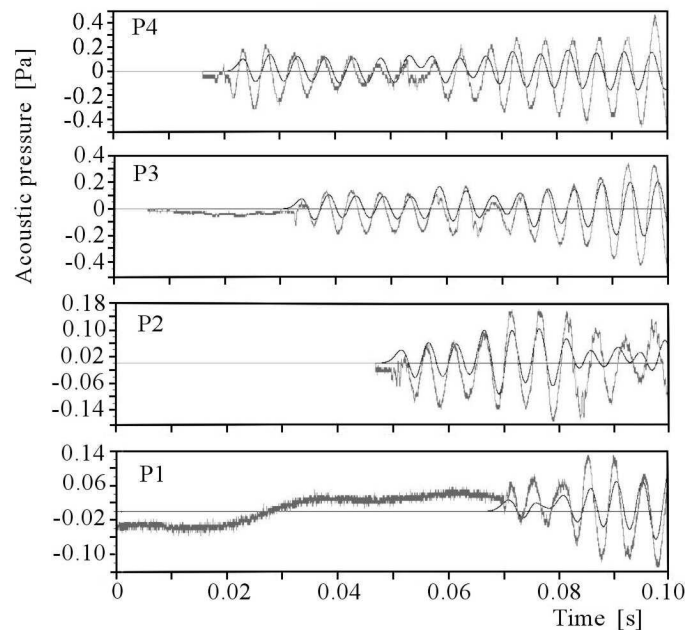

Fig. 11. Comparison for 200 Hz: experiment (grey line), numerical solution (black line)

In Fig. 11, the results of experimental tests and numerical analysis for the excitation frequency equal to 200 Hz are compared. The convergence of both the amplitude and phase of acoustic pressure is high in all measurement points. One should notice the number or finite elements per wavelength. The average dimensions of the finite element were ~ 0.1 m, so for 200 Hz there were nearly 17 elements per wavelength in the analysis.
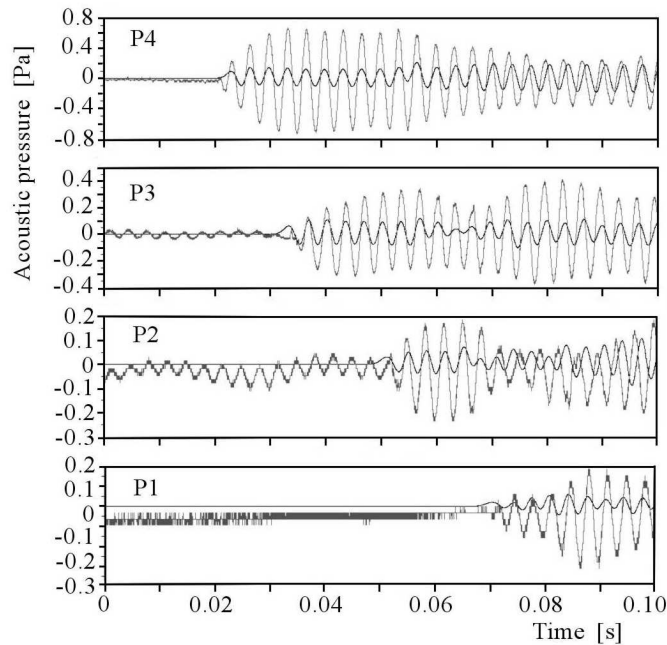
Fig. 12. Comparison for 300 Hz: experiment (grey line), numerical solution (black line)

The last sentence has a fundamental meaning. Comparisons made for other frequencies of interest showed that although the accuracy in phase is high enough, the convergence in amplitude of traveling waves decreases considerably. In Fig. 12 the results of experimental tests and numerical analysis for the excitation frequency equal to 300 Hz are compared. It is clearly visible that the convergence in amplitude was lost. By simple computations, we can determine the number of elements per wavelength just as before. Because of the mesh density, which did not change during the analysis, for 300 Hz there were around 11 elements per wavelength in the analysis.

For upper frequencies such effects were more and more sharply outlined.

5. Conclusions

Limitations in the application of FEM in acoustic analysis can be divided into three groups. The first group involves problems with proper choice of element sizes. The second group includes hardware problems, and the last one takes into account boundary difficulties.

A example of assembly hall "MAGNA" proved all the above mentioned limitations. It was clearly seen that the mesh density had fundamental meaning. Recommendations in relation to the minimal number of the finite elements per wavelength, introduced in Section 3.1 (based on [1]), are not adequate as the example of hall "MAGNA" had prowed. The results indicated that the maximal dimensions of element should be at least 10 times smaller then the acoustic wavelength.

A additional limitation was the fact that only a two dimensional model could be analysed. Because of this, the first run of the acoustic wave through the assembly hall could be recognized. But not only the conclusions about the convergence of the numerical and experimental results at measurement points could be done. The analysis of the contour maps, showing the rate of change of the acoustic pressure in the model (Fig. 9), had indicated that the shape of the first reflected wave was well matched to the amphitheatrical auditorium, so the uniform loudness should be inside.

In spite of the criticism to application of FEM in acoustic analysis, it has to be outlined that great meaning of the method in the field of acoustics is unquestionable, and is still growing along with hardware development.

References

1. ABAQUS Theory Manual, v6.5, 2005

2. Gołaś A., 1995, *Metody komputerowe w akustyce wnętrz i środowiska*, AGH, Kraków

3. Malecki I., 1969, *Physical Fundations of Technical Acoustics*, Oxford: Pergamon Press, Warszawa, PWN

4. Rabbiolo G., Bernhard R.J., Milner F.A., 2004, Definition of a high-frequency threshold for plates and acoustical space, *Journal of Sound and Vibrations*, **277**, 647-667

5. Reddy J.N., **1976**, *An Introduction to The Finite Element Method*, McGraw-Hill, USA

6. Sadowski J., 1971, *Akustyka w urbanistyce, architekturze i budownictwie*, Wyd. Arkady, Warszawa

7. SADOWSKI J., 1976, *Akustyka architektoniczna*, PWN, Warszawa

8. SADOWSKI J., WODZIŃSKI L., 1959, *Akustyka pomieszczeń*, Wydawnictwo Komunikacyjne

9. STRUTT J.W. (BARON RAYLEIGH), 1945, *The Theory of Sound*, Dover Publications, New York (originally published in 1877)

10. SUMELKA W., 2004, *Acoustics in Structural Engineering* (in Polish), M.Sc. Thesis, PUT, Poznań

11. SUMELKA W., ŁODYGOWSKI T., 2006, Substitute acoustic boundary impedance conditions for boundaries with periodic geometry in computer simulations of acoustic planar wave traveling, *Journal of Mechanical Engineering*, submitted

Ograniczenia zastosowania Metody Elementów Skończonych w analizie numerycznej pola akustycznego

Streszczenie

W pracy przedstawiono ograniczenia zastosowania Metody Elementów Skończonych w analizie numerycznej pola akustycznego. Wykazano, iż trudności w ocenie rozkładu akustycznych pól ciśnień spowodowane są doborem funkcji kształtu, wrażliwością na warunki brzegowe oraz gęstością stosowanych siatek MES. Na bazie porównania symulacji numerycznych z przeprowadzonym eksperymentem pokazano, w jaki sposób można niektóre z tych ograniczeń pominąć oraz do jakiego stopnia można uprościć analizę akustyczną, przyjmując modele dwuwymiarowe.